Cell. Mol. Life Sci. (2017) 74:3827–3840
DOI 10.1007/s00018-017-2552-7

Cellular and Molecular Life Sciences

ORIGINAL ARTICLE

OX40 promotes obesity-induced adipose inflammation and insulin resistance

Bing Liu[1,2,3] · Hengchi Yu[1,2,3] · Guangyong Sun[2,3,4] · Xiaojing Sun[2,3,4] · Hua Jin[2,3,4] · Chunpan Zhang[2,3,4] · Wen Shi[2,3,4] · Dan Tian[2,3,4] · Kai Liu[2,3,4] · Hufeng Xu[2,3,4] · Xinmin Li[2,3,4] · Jie Yin[1] · Xu Hong[1] · Dong Zhang[2,3,4]

Received: 18 December 2016 / Revised: 28 May 2017 / Accepted: 30 May 2017 / Published online: 13 June 2017

Abstract Adaptive immunity plays a critical role in IR and T2DM development; however, the biological mechanisms linking T cell costimulation and glucose metabolism have not been fully elucidated. In this study, we demonstrated that the costimulatory molecule OX40 controls T cell activation and IR development. Inflammatory cell accumulation and enhanced proinflammatory gene expression, as well as high OX40 expression levels on $CD4^+$ T cells, were observed in the adipose tissues of mice with diet-induced obesity. OX40-KO mice exhibited significantly less weight gain and lower fasting glucose levels than those of WT mice, without obvious adipose tissue inflammation. The effects of OX40 on IR are mechanistically linked to the promotion of T cell activation, Th1 cell differentiation and proliferation—as well as the attenuation of Treg suppressive activity and the enhancement of proinflammatory cytokine production—in adipose tissues. Furthermore, OX40 expression on T cells was positively associated with obesity in humans, suggesting that our findings are clinically relevant. In summary, our study revealed that OX40 in $CD4^+$ T cells is crucial for adipose tissue inflammation and IR development. Therefore, the OX40 signaling pathway may be a new target for preventing or treating obesity-related IR and T2DM.

Keywords Adipocyte · Adipose inflammation · Costimulation molecule · Diet-induced obesity · High-fat diet · IFN-γ · IL-17a · Immunology · Th1 · Th17 · Regulatory T cells

Abbreviations

APC	Antigen presenting cell
DIO	Diet-induced obesity
EdU	5-Ethynyl-2′-deoxyuridine
FACS	Fluorescence-activated cell sorting
Foxp3	Transcription factor forkhead box P3
Gata3	Transcription factor GATA binding protein 3
GTT	Glucose tolerance test
HBSS	Hanks' balanced salt solution
HE	Hematoxylin–eosin
HFD	High-fat diet
IL-2	Interleukin 2
IL-4	Interleukin 4
IL-6	Interleukin 6
IL-10	Interleukin 10
IL-17a	Interleukin 17a

Electronic supplementary material The online version of this article (doi:10.1007/s00018-017-2552-7) contains supplementary material, which is available to authorized users.

Bing Liu, Hengchi Yu and Guangyong Sun contributed equally to this work.

✉ Xu Hong
hxfriend@163.com

✉ Dong Zhang
zhangd2010@hotmail.com

[1] Endocrinology Department, Beijing Friendship Hospital, Capital Medical University, Beijing 100050, People's Republic of China

[2] Experimental and Translational Research Center, Beijing Friendship Hospital, Capital Medical University, No. 95 Yong-an Road, Xi-cheng District, Beijing 100050, People's Republic of China

[3] Beijing Key Laboratory of Tolerance Induction and Organ Protection in Transplantation, Beijing 100050, People's Republic of China

[4] Beijing Clinical Research Institute, Beijing 100050, People's Republic of China

IFN-γ	Interferon-γ
IR	Insulin resistance
ITT	Insulin tolerance test
KO	Knockout
mAb	Monoclonal antibody
MHC-II	MHC class II
NCD	Normal control diet
NKT	Natural killer T cells
PBMC	Peripheral blood mononuclear cell
T2DM	Type 2 diabetes mellitus
Tbx21	T-box transcription factor TBX21
Th1	T helper 1
TNF-α	Tumor necrosis factor alpha
Tregs	T regulatory cells
VAT	Visceral adipose tissue
WT	Wide type

Introduction

Obesity-related insulin resistance (IR) and type 2 diabetes mellitus (T2DM) have become worldwide public health issues. Adipose tissue inflammation is a causal link between obesity and IR, and proinflammatory cell accumulation in visceral adipose tissue (VAT) plays a fundamental role in IR development and its progression to T2DM [1–4]. Both innate and adaptive immunity actively participate in the highly complex regulation of adipose tissue and modulate inflammatory and metabolic cascades in all stages of obesity [5–8].

The crosstalk between the innate and adaptive immune systems in VAT is crucial for obesity-related IR and T2DM development and progression [9]. Adipose tissue promotes T helper 1 (Th1) $CD4^+$ T cell activation during the early stages of diet-induced obesity (DIO) in obese animals, prior to monocyte/macrophage infiltration [7, 10], suggesting that MHC class II (MHC-II)-expressing adipocytes trigger $CD4^+$ T cell activation and differentiation in the early stages of obesity. IFN-γ-secreting T cells (Th1) enhance monocyte recruitment and differentiation into proinflammatory macrophages, which release IL-1, IL-6 and TNF-α [11] and impair insulin sensitivity in adipocytes. Macrophages regulate $CD4^+$ T cell activation and differentiation during obesity-related IR and T2DM [12–15].

$CD4^+$ T cell activation requires MHC-II-dependent antigen presentation on antigen-presenting cells (APCs), as well as the presence of costimulatory molecules. After a T cell receptor (TCR) binds to an MHC-II molecule, costimulatory molecules induce the $CD4^+$ T cells and APCs to initiate immune responses [16]. Costimulatory interactions likely mediate extensive crosstalk between innate and adaptive immunity during the pathogenesis of obesity and obesity-related complications. The crosstalk between B7-CD28 or CD40–CD40L plays a dual role in DIO development by inducing protective regulatory T cell responses and eliciting effector T cell proinflammatory functions [9]. OX40, an important costimulatory molecule, is important for promoting T cell (especially $CD4^+$ T cells) clonal expansion and differentiation and, ultimately, long-lived memory cell generation [17]. However, its role in obesity-related IR and T2DM development and progression has not been explored.

In this study, we elucidated the proinflammatory role of the costimulatory molecule OX40 in a DIO model using OX40-knockout (OX40-KO) mice and investigated the mechanism by which OX40 induces IR.

Materials and methods

Animal protocol

Age (8 weeks old) and weight matched male wild-type (WT) C57BL/6, C57BL/6 OX40-KO, C57BL/6 congenic for CD45.1 and B6.Rag2/Il2rg double knock mice were purchased from The Jackson Laboratory (Bar Harbor, ME, USA). These mice received either a normal control diet (NCD) or a high-fat diet (HFD, 45 kcal% fat, Beijing HFK Bioscience, Beijing, China) beginning at 8 weeks of age. The mice were maintained in a pathogen-free, temperature-controlled environment under 12 h light/dark cycles at Beijing Friendship Hospital, and all protocols were approved by the Institutional Animal Care and Ethics Committee.

Reagent and antibodies

Bead arrays for mouse IFN-γ, TNF-α, and IL-6 were purchased from BD Biosciences (San Diego, CA, USA). Fluorochrome-conjugated antibodies against mouse CD11b, CD3, CD4, CD8, CD45, CD69, NK1.1, TCRβ, OX40, Foxp3, IFN-γ, and OX40L and human OX40 and OX40L were obtained from eBioscience (San Diego, CA, USA).

Intraperitoneal glucose tolerance test (GTT) and insulin tolerance test (ITT)

GTT and ITT were performed after 6-h fast. For GTT, mice were injected intraperitoneally with 1 g/kg D-glucose. For ITT, mice were injected with 0.75 units/kg regular human insulin (Humulin R, Lilly). Blood samples were collected before and 30, 60, 90, and 120 min after the insulin or glucose injection. Plasma glucose concentration was measured with Medisaff (Terumo Corporation, Japanese). Insulin

plasma levels were quantified by Mouse Insulin ELISA Kit (Merck Millipore Corporation, Billerica, MA, USA).

T cell isolation and T cell proliferation assay

Splenocytes from WT and OX40-KO mice were stained with anti-CD3, CD4, CD8, TCRβ and NK1.1 monoclonal antibodies (mAb). $CD3^+$ T cells ($CD3^+TCR\beta^+NK1.1^-$), $CD4^+$ T cells ($CD3^+TCR\beta^+CD4^+NK1.1^-$) and $CD8^+$ T cells ($CD3^+TCR\beta^+CD8^+NK1.1^-$) were purified via cell sorting. Purified T cell subsets were cultured in triplicate in wells pre-coated with anti-CD3 mAb (3 μg/mL, Clone: 145-2C11, BD Biosciences) and soluble anti-CD28 mAb (1 μg/mL, Clone: 37.51, BD Biosciences) at 37 °C with 5% CO_2. After 72 h of incubation and 12 h before harvesting, 5-ethynyl-2′-deoxyuridine (EdU) was added to the plates (final concentration was 50 μM). Cell proliferation was measured via EdU incorporation, according to the manufacturer's instructions (EdU staining kit, RiboBio Corporation, Guangzhou, China).

In vitro Treg suppression assay

$CD3^+$ T cells (3×10^5 cells/well) enriched by T cell enrichment columns from the splenocytes of CD45.1 C57BL/6 mice were incubated with 3 μg/mL anti-CD3 (Clone: 145-2C11) antibodies and syngeneic APCs (3×10^5 mitomycin C-treated splenocytes from WT C57BL/6 mice) and cultured with or without Tregs ($CD4^+CD25^{high}CD127^-$, $Foxp3^+$ purity >95%) from HFD-fed WT or OX40-KO mice at a ratio of 4:1 in 96-well flat-bottom culture plates. After 3 days, CD45.1-positive cell EdU incorporation was determined via flow cytometry.

In vitro leptin stimulation assay

Naïve T effector cells (Teff, $CD4^+CD25^-$ T cells) were isolated from the splenocytes of WT C57BL/6 or OX40-KO mice and then stimulated with anti-CD3 (3 μg/mL, Clone: 145-2C11, BD Biosciences) and anti-CD28 (2 μg/mL Clone: 37.51, BD Biosciences) antibodies with or without recombinant mouse leptin (5 μg/mL). Two days later, $CD4^+$ T cells were collected for Tbx21 and Gata3 mRNA analyses by real-time PCR.

In vitro IFN-γ stimulation assay

Visceral adipose tissue mononuclear cells from naïve C57BL/6 mice were cultured with 10 ng/mL recombinant mouse IFN-γ (Peprotech, Rocky Hill, NJ, USA). 12 and 24 h later, the cells were collected for proinflammatory cytokine mRNA analyses by real-time PCR.

Adoptive transfer of T cells

CD3 T cells (5×10^6, purity >97%) were sorted from splenocytes of WT C57BL/6 or OX40-KO mice, and transferred into B6.Rag2/Il2rg double knock mice by tail vein injection. Recipient animals subsequently consumed HFD for 16 weeks.

Real-time PCR

Total RNA was isolated from splenocytes or epididymal fat pads using an RNeasy Plus Mini Kit (Qiagen, Valencia, CA, USA) and reverse transcribed to cDNA using a SuperScript III RT-kit (Invitrogen, Carlsbad, CA, USA). *OX40, OX40L, Foxp3, Tbx21, RORγT, Gata3, Tnfa* (*TNF-α*), *Ifng* (*IFN-γ*), *Il6* (*IL-6*), *Ccl2*, *Cxcl9, NKp46* and *Leptin* mRNA levels were quantified by real-time PCR using an ABI 7500 Sequence Detection System (Applied Biosystems, Foster City, CA, USA). Amplicon expression in each sample was normalized to *GAPDH*. After normalization, gene expression was quantified using the $2^{-\Delta\Delta C_t}$ method. The primer sequences are shown in Supplementary Table 1.

Flow cytometry analysis

Peripheral blood, splenic and VAT mononuclear cells were harvested and analyzed to determine the expression levels of various cell-surface markers. All samples were acquired on a FACSAria II flow cytometer (BD Biosciences, CA, USA), and the data were analyzed using FlowJo software (Treestar, Ashland, OR, USA).

Clinical study

For the observational study, we evaluated 140 patients visiting the Physical Examination Center of Beijing Friendship Hospital for routine physical examinations. All subjects were required to be nondiabetic, which was defined as a fasting serum glucose <6.1 mmol/L, and free of major organ disease, chronic inflammatory conditions, cancer, active psychiatric diseases and a history of surgery. All subjects provided written informed consent to participate in the study, whose protocol was approved by the Human Institutional Review Board of Beijing Friendship Hospital. Peripheral blood mononuclear cells (PBMCs) were collected in vacutainer tubes. Fasting serum glucose, cholesterol and triglyceride levels were measured using standard laboratory techniques. OX40 expression on T cells was tested via flow cytometry, and the OX40 and OX40L mRNA levels in PBMCs were quantified via real-time PCR.

Statistics

Statistical analysis was performed with SPSS (SPSS Inc). Values are expressed as the mean ± standard deviation (SD). Significances in GTT and ITT were assessed by repeated-measures two-way ANOVA. Significant differences were analyzed using Student's *t* test and one-way ANOVA. In the clinical study, the normal distribution of variables was tested with the Shapiro–Wilk test. Differences between groups were compared by *t* test for normal variables and Mann–Whitney test for nonnormal variables. p values <0.05 were considered significant.

Results

HFD-induced obese mice exhibit increased OX40 expression in adipose tissues and splenic T cells

To investigate the role of the costimulatory molecule OX40 in DIO and T2DM, we fed C57BL/6 mice HFDs or NCDs. As expected, HFD-fed mice experienced significant weight gains and fasting glucose level increases. Mononuclear cells isolated from the epididymal VAT and splenic tissues of mice fed either NCDs or HFDs for 16 weeks were used for flow cytometric OX40 detection.

Compared with the NCD-fed control mice, HFD-fed mice exhibited upregulated OX40 expression on T cells in both VAT and splenic tissues (Fig. 1a), the gating strategy used for flow cytometry is shown in supplementary figure S1. HFD-fed mice also exhibited significantly increased splenic $CD3^+$ T cell (13.630 ± 0.742% in the HFD group vs. 8.570 ± 1.281% in the NCD group, $p = 0.0235$), $CD4^+$ T cell (15.167 ± 1.513% in the HFD group vs. 9.060 ± 0.584% in the NCD group, $p = 0.0285$) and $CD8^+$ T cell OX40 levels (14.230 ± 1.868% in the HFD group vs. 8.883 ± 1.436% in the NCD group, $p = 0.0487$) and substantially increased epididymal VAT total $CD3^+$ T cell (15.900 ± 0.322% in the HFD group vs. 11.367 ± 0.816% in the NCD group, $p = 0.0003$) and $CD4^+$ T cell OX40 levels (13.467 ± 0.393% in the HFD group vs. 7.077 ± 0.194% in the NCD group, $p = 0.0001$). However, HFD-fed mice did not exhibit significant increases in VAT epididymal $CD8^+$ T cell levels (19.733 ± 3.295% in the HFD group vs. 14.467 ± 1.506% in the NCD group, $p = 0.1039$) (Fig. 1b).

OX40 expression levels were strikingly increased by 1.9- and 1.4-fold on the epididymal VAT and splenic $CD4^+$ T cells, respectively, of HFD-fed mice compared with those on the epididymal VAT and splenic $CD4^+$ T cells of lean mice (Fig. 1c). Relative *OX40* and *OX40L* mRNA expression levels were also upregulated in the VAT and splenic tissues of HFD-fed mice compared with those of lean mice (Fig. 1d). The correlation between OX40 expression and DIO suggests that OX40 on T cells, especially $CD4^+$ T cells, is involved in HFD-induced obesity and IR.

OX40-deficient mice are protected against HFD-induced glucose homeostasis impairments

To determine the potential role of OX40 in inflammation and IR regulation in DIO, we fed WT and OX40-KO mice either NCDs or HFDs. As shown in Fig. 2a, no significant difference of body weight between WT and OX40-KO mice fed with NCDs was observed. However, HFD-fed OX40-KO mice gained significantly less weight than age-matched HFD-fed WT mice (Fig. 2a), and this correlated with significantly lowered the percentage of epididymal fat weight relative to total body weight (Fig. 2b), decreased adipocyte size and lymphocyte adipose infiltration (Fig. 2c). Compared with WT control mice, OX40-KO mice fed HFDs for 16 weeks exhibited significantly lower fasting blood glucose levels than those of WT mice fed HFDs for the same amount of time (Fig. 2d) (OX40-KO 8.350 ± 0.381 vs. WT 10.58 ± 0.349 mmol/L, $p = 0.0237$). HFD-fed OX40-KO mice also exhibited significantly decreased fasting insulin levels compared with those of HFD-fed WT mice (Fig. 2e) (OX40-KO 0.396 ± 0.037 ng/mL vs. WT 1.203 ± 0.252 ng/mL, $p = 0.0194$). After 16 weeks of HFD feeding, the mice in each group were subjected to GTTs and ITTs, HFD-fed OX40-KO mice exhibited improved glucose tolerance and insulin sensitivity compared to that of HFD-fed WT obese controls (Fig. 2f, g). These mice also displayed deficient epididymal VAT *leptin* mRNA expression compared with that of their WT counterparts (Fig. 2h).

To further approve that OX40 expression on T cells contributes to the phenotype observed in OX40-KO mice, we selectively repopulated B6.Rag2/Il2rg double knock mice with purified CD3 T cells from WT or OX40-KO mice. After 16 weeks HFD feeding, the mice transferred with OX40 deficient CD3 T cells showed remarkably lowered body weight than age-matched recipient mice adoptive transferred with WT CD3 T cells, with decreased fasting glucose levels in plasma (Supplementary Fig. S2). Taken together, these findings indicate that T cell OX40 upregulation promotes DIO and IR.

OX40 deficiency suppresses $CD4^+$ T cell activation and prevents macrophage infiltration in the adipose tissues of obese mice

Proinflammatory T cell and macrophage infiltration of VAT directly contributes to obesity-related IR [18]. Thus, to elucidate the mechanisms underlying the IR

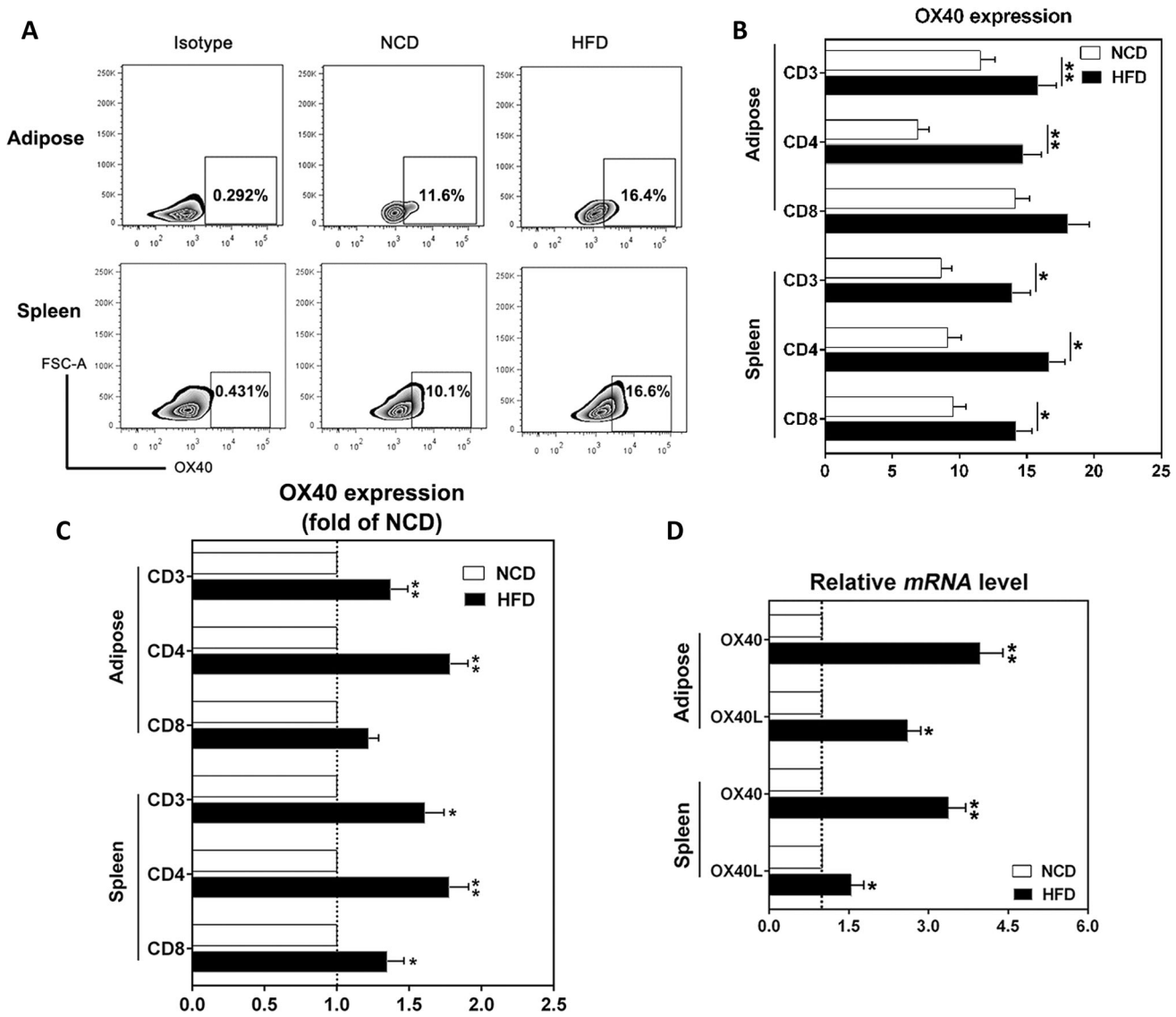

Fig. 1 OX40 expression was increased in the adipose tissue and splenic T cells of HFD-fed obese mice. Mononuclear cells isolated from the epididymal VAT and splenic tissue of mice fed either an NCD or an HFD for 16 weeks were used to detect OX40 via flow cytometric analysis. **a** Representative flow cytometry image of OX40 expression on $CD3^+$ T cells. **b** Statistical analysis of OX40 expression on VAT and splenic $CD3^+$, $CD4^+$ and $CD8^+$ T cells, which was measured via flow cytometry. **c** Relative changes in OX40 expression induced by HFD administration were plotted as fold changes of OX40 expression induced by NCD administration. **d** Relative *OX40* and *OX40L* mRNA levels in the adipose and splenic tissues of obese mice. The data are presented as the mean ± SD, $n = 5$ in each group. $^*p < 0.05$, $^{**}p < 0.01$

amelioration observed in OX40-KO mice during HFD feeding, we determined the immune cell compositions of OX40-KO and WT mouse epididymal VAT, splenic tissue, and peripheral blood. Compared with WT mice, OX40-KO mice exhibited substantially reduced epididymal VAT and peripheral blood $CD11b^+$ cell (Fig. 3a). In epididymal VAT, the percentage of M1 macrophages ($CD11b^+F4/80^+CD11C^+$) relative to the total numbers of infiltrated macrophages in OX40-KO mice was strikingly decreased (Fig. 3b). OX40-KO mice also exhibited substantially reduced epididymal VAT and peripheral blood $CD3^+$ T cell (Fig. 3c, d), $CD4^+$ T cell (Fig. 3e) and $CD8^+$ T cell (Fig. 3f) levels. Obese OX40-KO mice also exhibited dramatic decreases in splenic $CD4^+$ T cell levels (Fig. 3e), as well as decreases in splenic and adipose tissue $CD69^+$ T cell levels (Fig. 4a). HFD-fed OX40-KO mice had significantly decreased $CD4^+CD69^+$ T cell percentages (WT 30.830 ± 3.477% vs. OX40-KO 5.523 ± 0.535% of total $CD4^+$ T cells; $p = 0.0001$) and $CD4^+CD44^+$ T cell percentages (WT 32.600 ± 1.809% vs. OX40-KO 21.900 ± 1.541% of total $CD4^+$ T cells; $p = 0.0041$), but not significantly decreased $CD8^+CD69^+$ T cell percentages

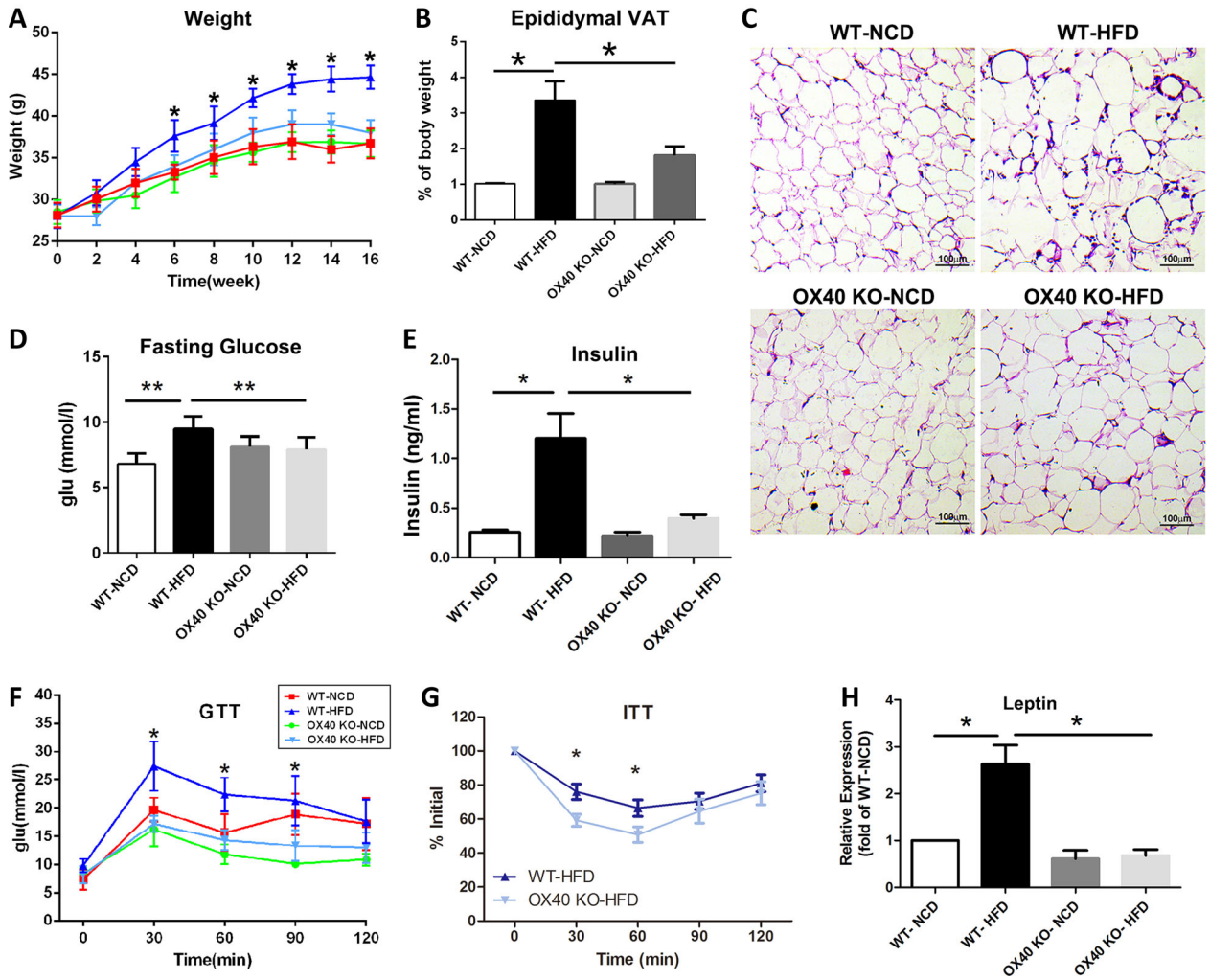

Fig. 2 OX40 deficiency ameliorated metabolic syndrome in mice. WT and OX40-KO mice were fed HFDs for 16 weeks and then compared with WT mice fed NCDs. Increases in body weight in each group are shown at the indicated time points (**a**). The adiposity was evaluated by the percentage of epididymal fat weight relative to total body weight (**b**). Representative epididymal VAT histology with the scale bar is set at 100 μm (**c**). Plasma glucose (**d**) and insulin (**e**) levels were measured after the animals had fasted for 6 h. GTT (**f**) and ITT (**g**) were performed after intraperitoneal glucose injection. Relative *leptin* expression in the epididymal VAT of each group was compared (**h**). The data are depicted as the mean ± SD, $n = 6$ in each group. *$p < 0.05$, **$p < 0.01$

(WT 15.270 ± 0.723% vs. OX40-KO 14.630 ± 0.367%, $p = 0.2259$) and $CD8^+CD44^+$ T cell percentages (WT 36.633 ± 0.327% vs. OX40-KO 35.567 ± 0.330%, $p = 0.0616$) in adipose tissue (Fig. 4a; Supplementary Fig. S3A).

To evaluate the differences in T cell activation and proliferation between OX40-KO mice and WT mice, we isolated splenocytes from each group of mice and incubated them with anti-CD3/CD28 antibodies. As shown in Fig. 4b, after 3 days of incubation, HFD-fed WT mice exhibited greater cell proliferation than that of NCD-fed mice. OX40 deletion suppressed T cell division, even in mice receiving HFDs. HFD-fed WT mice exhibited strong $CD4^+$ and $CD8^+$ T cell proliferation. HFD-fed OX40-KO mice exhibited decreased $CD4^+$ T cell proliferation but not decreased $CD8^+$ T cell proliferation (Fig. 4c). These data indicate that OX40 deficiency significantly suppressed T cell activation and proliferation, especially $CD4^+$ T cell activation and proliferation. Therefore, OX40 deficiency represents a T cell anti-inflammatory phenotype.

OX40 deficiency significantly decreases and thus rebalances the Th1/Treg ratio in adipose tissue during HFD administration

To investigate the potential mechanism underlying the contributions of OX40 to adipose tissue inflammation, we evaluated VAT and splenic T cell phenotypes. HFD-fed

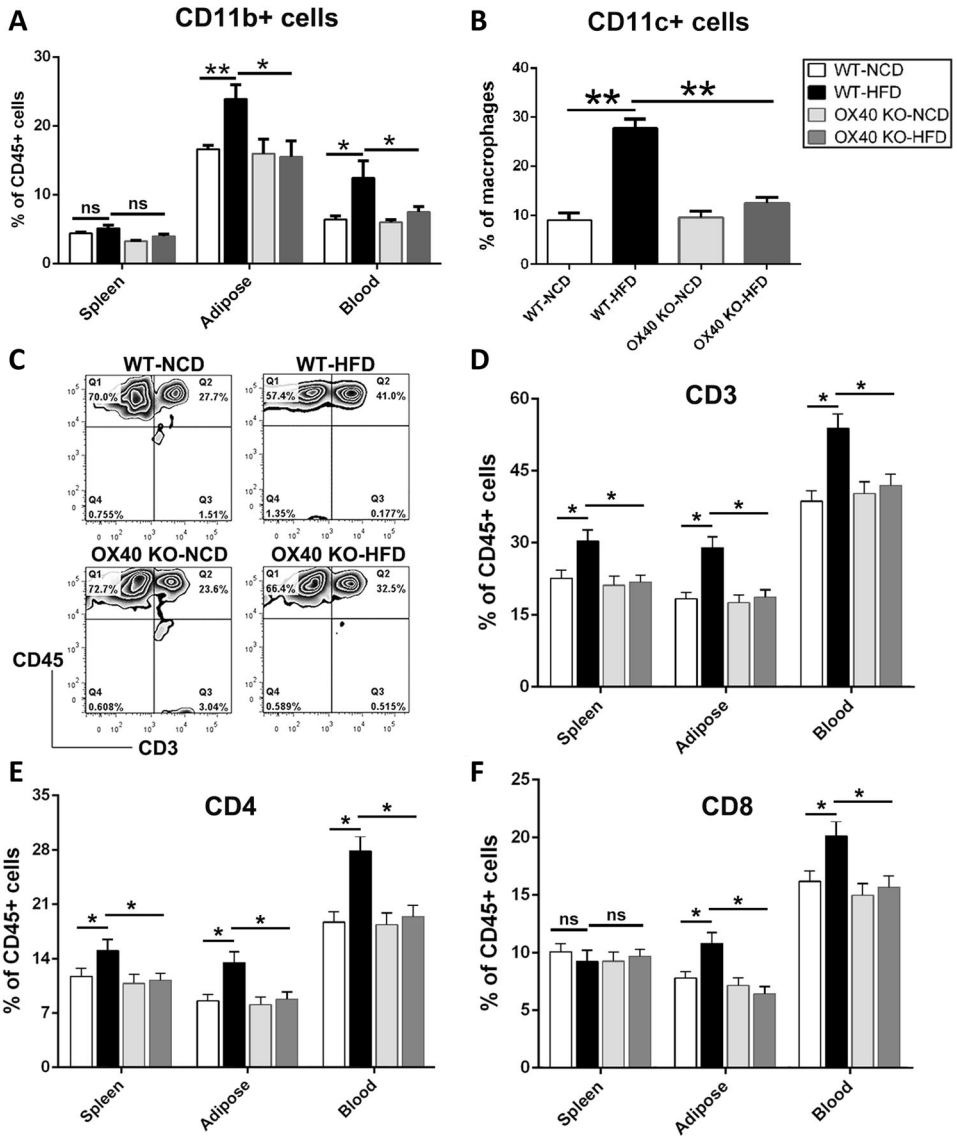

Fig. 3 OX40 deficiency decreased immune cell infiltration in adipose tissues. Leukocyte subsets in adipose tissue were characterized via flow cytometry. **a** $CD45^+$ leukocytes were gated for analysis of $CD11b^+$ macrophages (% leukocytes) in the adipose tissue, splenic tissue and blood of WT and OX40-KO mice. **b** The percentage of M1 macrophages ($CD11b^+F4/80^+CD11C^+$) relative to the total numbers of macrophages infiltrated in epididymal VAT in each group was compared. **c** Representative flow cytometry image of $CD3^+$ T cells (% leukocytes) in the splenic tissues of mice in each group. Statistical analysis of $CD3^+$ T cell (**d**), $CD4^+$ T cell (**e**) and $CD8^+$ T cell (**f**) (% leukocytes) levels in the splenic tissue, adipose tissue and peripheral blood of mice from each group, as determined by flow cytometry. The data are depicted as the mean ± SD, $n = 5$ in each group. $^*p < 0.05$, $^{**}p < 0.01$, *ns* no significance

mice exhibited significantly increased proportions of IFN-γ-producing cells and Foxp3-positive cells relative to the total numbers of CD4 T cells, while OX40-KO mice exhibited decreased proportions of IFN-γ-producing cells and Foxp3-positive cells relative to the total numbers of CD4 T cells (Fig. 5a).

HFD-fed mice exhibited significantly increased proportions and of IFN-γ-producing $CD4^+$ T cells and Foxp3-positive $CD4^+$ T cells in both epididymal VAT and spleen, while HFD-fed OX40-KO mice had substantially decreased percentages of IFN-γ-producing cells (WT 12.650 ± 1.466% vs. OX40-KO 6.490 ± 0.170% of total $CD4^+$ T cells in VAT, $p = 0.0194$; WT 8.687 ± 0.473% vs. OX40-KO 4.337 ± 0.038% of total $CD4^+$ T cells in spleen; $p = 0.0008$) and Foxp3-positive cells in these tissues (WT 12.900 ± 0.473% vs. OX40-KO 10.970 ± 0.088% of total $CD4^+$ T cells in VAT, $p = 0.0158$; WT 21.830 ± 0.914% vs. OX40-KO 15.070 ± 0.376% of total $CD4^+$ T cells in spleen; $p = 0.0024$) (Fig. 5b). HFD-fed mice exhibited higher proportions of IFN-γ-producing $CD8^+$ T cells in VAT but not in splenic tissue. HFD-fed OX40-KO mice also displayed slightly decreased proportions of IFN-γ-producing $CD8^+$ T cells in VAT compared to HFD-fed WT mice (WT 5.800 ± 0.892% vs. OX40-KO 3.847 ± 0.492% of total $CD3^+$ T cells in VAT; $p = 0.1277$). The absolute counts of Th1 ($CD4^+IFN\text{-}\gamma^+$ T cells) and Treg ($CD4^+Foxp3^+$ T cells) in VAT and spleen were also evaluated, HFD-fed mice exhibited significantly increased number of Th1 and Treg, while HFD-fed OX40-KO mice had substantially decreased Th1 and Treg (Supplementary Fig. S3B). Thus, HFD administration-induced significant Th1/Treg ratio increases, while OX40 knockout in $CD4^+$ T cells significantly decreased and thus rebalanced the Th1/Treg ratio (Fig. 5c).

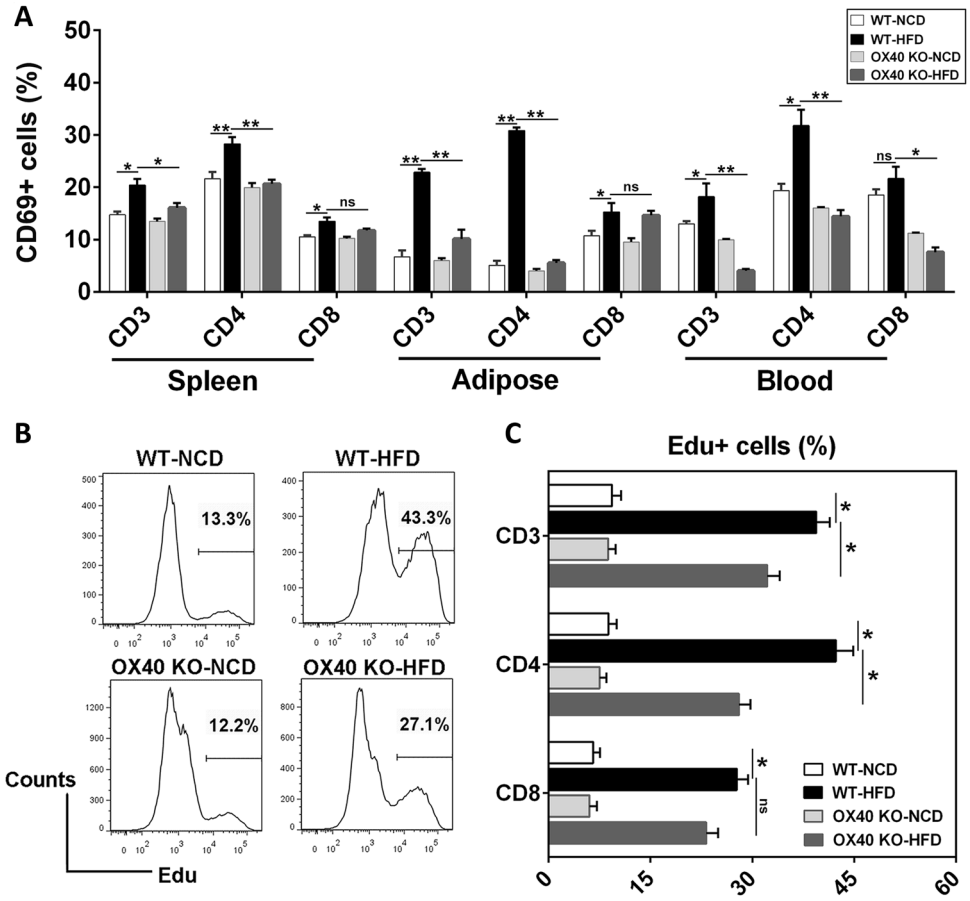

Fig. 4 OX40 deficiency dampened $CD4^+$ T cell activation and proliferation. The percentages of $CD69^+$ cells relative to the total numbers of $CD3^+$, $CD4^+$ and $CD8^+$ T cells were determined by flow cytometry in the indicated groups ($n = 5$ in each group) (**a**). Splenocytes isolated from each group were incubated with anti-CD3/CD28 antibodies for 3 days, and proliferation was assessed via EdU incorporation. Representative flow cytometry image of EdU^+ cells (% $CD3^+$ T cells) from each group (**b**). Statistical analysis of EdU^+ cells relative to the total numbers of $CD3^+$ T cells, $CD4^+$ T cells and $CD8^+$ T cells in each group, as determined by flow cytometry (**c**). The data are depicted as the mean ± SD, $n = 3$ in each group. $*p < 0.05$, $**p < 0.01$, *ns* no significance

Furthermore, we subsequently quantified Th lineage-defining transcription factor and proinflammatory cytokine expression by real-time PCR. As shown in Fig. 5d, HFD-fed mice displayed significantly upregulated transcription factor (*Tbx21, RORγT* and *Foxp3*, but not *Gata3*) and proinflammatory cytokine gene expression (*Tnfa, Ifng* and *Il6*) in adipose tissue, while HFD-fed OX40-KO mice exhibited significantly lower levels of *Tbx21, Foxp3, Tnfa, Ifnr* and *Il6* in adipose tissue. A trend toward a decrease in *RORγT* mRNA expression was also noted from HFD-fed OX40-KO mice, although no statistical significance was observed. However, flow cytometry data showed that HFD-fed OX40-KO mice had remarkably decreased IL-17 but not IL-4 producing $CD4^+$ T cells in VAT (Supplementary Fig. S3C). Taken together, these findings indicate that OX40 deficiency suppressed CD4 T cells toward Th1 and Th17 differentiation.

OX40 deficiency suppresses leptin-induced Th1 differentiation and maintains Treg suppressive activity and adipose tissue homeostasis

Leptin reportedly stimulates IFN-γ secretion [10, 19]. To investigate the role of OX40 in T cell differentiation in obese mice, we incubated naïve $CD4^+CD25^-$ T cells (T effector cells, Teff) from the splenocytes of either WT or OX40-KO mice with anti-CD3/CD28 antibodies and leptin. As shown in Fig. 6a, b, compared with $CD4^+$ T cells incubated with anti-CD3/CD28 alone, $CD4^+$ T cells incubated with leptin exhibited marked increases in *Tbx21* and *Ifng* expression. OX40 knockout resulted in significantly downregulated *Tbx21* and *Ifng* expression in $CD4^+$ T cells. These results suggest that adipocyte-derived leptin can stimulate naïve $CD4^+CD25^-$ T cells to differentiate into Th1 cells and that OX40 enhances Th1 polarization. To confirm that IFN-γ-producing Th1 cells stimulated by leptin contribute to adipose inflammation, we quantified proinflammatory cytokine expression in adipose tissue via real-time PCR 24 and 48 h after IFN-γ stimulation in vitro (Fig. 6b). As expected, IFN-γ upregulated *Cxcl9, Tnfa, Ifng, Ccl2* and *Il6* expression.

To investigate the effects of OX40-OX40L signaling on Treg suppressive activity, we performed an in vitro suppression assay. Tregs from both HFD-fed WT and OX40-KO mice suppressed anti-CD3-stimulated naïve $CD4^+$ T cell proliferation, and no difference in $CD4^+$ T cell proliferation was observed when Tregs and $CD4^+$ T cells were

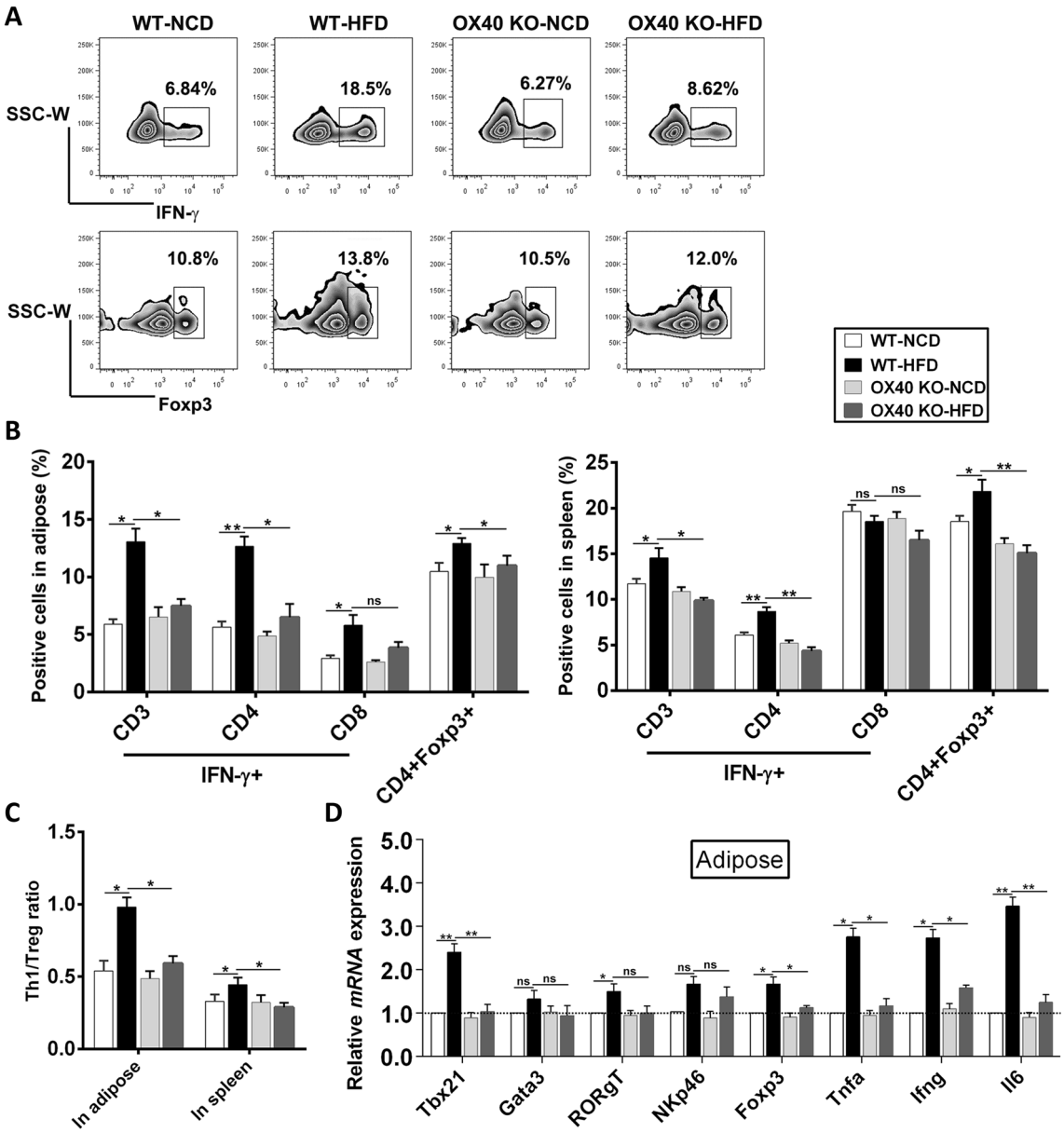

Fig. 5 OX40 deficiency rebalanced the Th1/Treg ratio in adipose tissue during HFD feeding. **a** Flow cytometry analysis of IFN-γ^+ cells and Foxp3$^+$ cells relative to the total numbers of CD3$^+$ T cells in the adipose tissue of mice from each group, expressed as lymphocyte percentages. **b** Changes in the percentages of IFN-γ^+ cells and Foxp3$^+$ cells relative to the total percentage of CD3$^+$, CD4$^+$ and CD8$^+$ T cells (quantified by flow cytometry) in the adipose tissue and splenic tissue of HFD-fed WT and OX40-KO mice were plotted. **c** Th1/Treg ratios were calculated as CD4$^+$IFN-γ^+/CD4$^+$Foxp3$^+$ relative to the total percentage of CD4$^+$ T cells (determined by flow cytometry) in the adipose tissue and splenic tissue of mice in each group. **d** Quantitative real-time PCR analysis of proinflammatory cytokine (*Tnfa, Ifng and Il6*) and transcription factor (*Tbx21, Gata3, RORγT* and *Foxp3*) levels in the adipose tissues of mice from each group. The data are presented as the mean ± SD, $n = 5$ in each group. *$p < 0.05$, **$p < 0.01$, *ns* no significance

cultured at a 1:1 ratio. However, when Tregs and CD4$^+$ T cells were cultured at a 1:4 ratio, HFD-fed OX40-KO mouse Tregs exhibited pronounced suppressive activity compared with that of HFD-fed WT mouse Tregs ($p = 0.04$, Fig. 6c, d), suggesting that OX40 upregulation on Tregs partially affects Treg suppressive activity in HFD-fed mice. Taken together, these findings indicate that the upregulation of OX40 contributes to adipose tissue inflammation and IR by promoting Th1 differentiation and inhibiting Treg suppressive activity.

OX40 is associated with obesity in humans

To determine if our findings are relevant for humans, we analyzed 140 patients with different body mass indices (BMIs) who visited the Physical Examination Center for

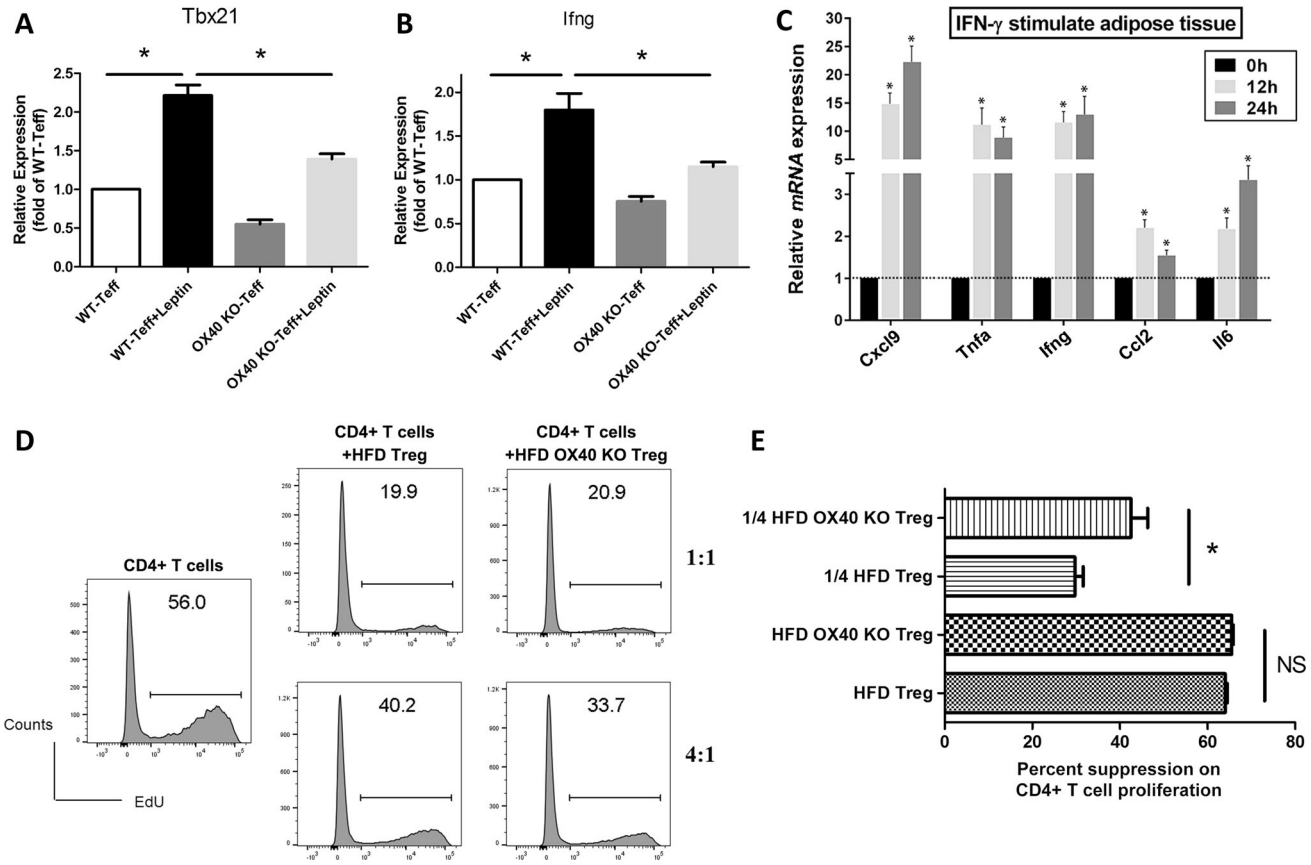

Fig. 6 OX40 deficiency rebalanced the Th1/Treg ratio in adipose tissue, suppressed Th1 cell differentiation, and maintained Treg and adipose homeostasis. Naïve $CD4^{+}CD25^{-}$ T cells from the splenocytes of either WT or OX40-KO mice were stimulated with anti-CD3/CD28 antibodies and leptin for 3 days. Relative *Tbx21* (**a**) and *Ifng* (**b**) expression levels in each group were compared. **c** Adipocytes isolated from each group were stimulated by recombinant IFN-γ in vitro for 12 or 24 h. Quantitative real-time PCR analyses of proinflammatory cytokine and chemokine mRNA levels in adipocytes were performed after in vitro stimulation. **d** Naïve T cells were stimulated with anti-CD3 antibodies and syngeneic APCs for 3 days. Tregs from HFD-fed WT and OX40-KO mice were mixed with naïve T cells at different ratios, and $CD4^{+}$ T cell proliferation suppression was observed. The data shown are representative of three individual experiments. **e** The suppressive effects of Tregs on naïve $CD4^{+}$ T cells in each group were compared. The data are depicted as the mean ± SD, $n = 3$ in each group. $^{*}p < 0.05$, $^{**}p < 0.01$, *ns* no significance

routine physical examinations in this observation study. Their demographic and clinical characteristics are shown in Supplementary Table 2. Patients were classified as obese or nonobese according to their BMIs (obese, $\geq$28 kg/m^2). PBMCs collected from lean and obese humans were subjected to flow cytometric testing to detect OX40 expression. mRNA isolated from the PBMCs of each patient was used to evaluate OX40 and OX40L expression. Notably, we detected higher OX40 expression levels on $CD3^{+}$ T cells, $CD4^{+}$ T and $CD8^{+}$ T cells in obese individuals with a high BMI (BMI $\geq$28) via flow cytometry (Fig. 7a). *OX40* and *OX40L* mRNA levels were also markedly increased in obese patients compared with those of lean controls (Fig. 7b), suggesting that OX40 and OX40L play a role in obesity-induced IR pathogenesis.

Discussion

Adaptive immunity has emerged as an important regulator of obesity-related adipose tissue inflammation, which suggests that it plays a critical role in glucose metabolism [20, 21]. Macrophage activation and polarization into the proinflammatory "M1" or anti-inflammatory "M2" phenotype are crucial for adipose tissue inflammation and are mediated by adaptive immune cells. $CD4^{+}$ T cell activation and differentiation in adipose tissue initiate crosstalk between adaptive and innate immunity in DIO and IR. Th1 and Th17 cells release IFN-γ and IL-17, which stimulate proinflammatory M1 macrophage differentiation, whereas Th2 cells and Tregs promote anti-inflammatory M2 macrophage differentiation via IL-4, IL-10 or IL-13 production [3, 6, 20, 21]. Thus, increases in the Th1/Treg or Th1/Th2

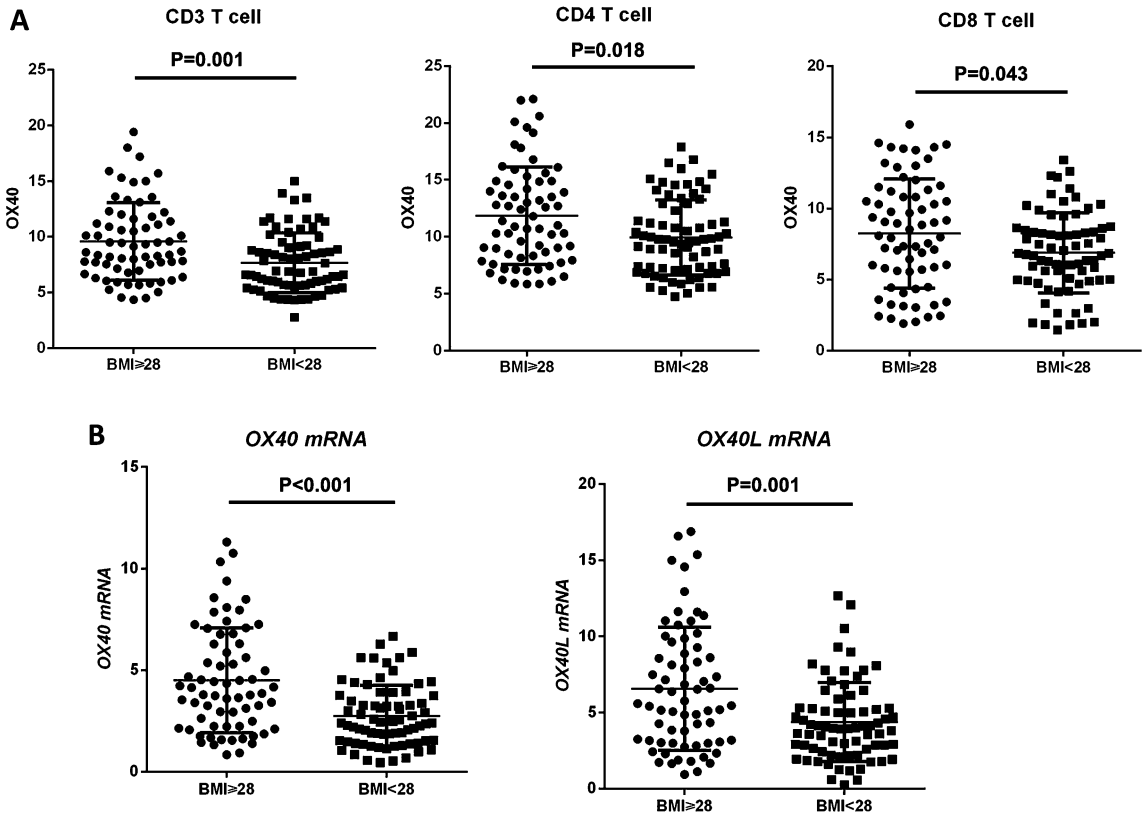

Fig. 7 OX40 is associated with obesity in humans. **a** PBMCs collected from 140 patients were used to detect OX40 expression on T cells via flow cytometry and plotted against the BMIs of the tested individuals. **b** PBMC RNA was extracted and tested for *OX40* and *OX40L* mRNA expression and plotted against the BMIs of the tested individuals. The data are depicted as the mean ± SD. *p* values are indicated in each graph

ratio in DIO induce adipose tissue inflammation by promoting macrophage differentiation to the proinflammatory M1 phenotype.

$CD4^+$ T cell activation requires costimulation in addition to MHC-II antigen presentation. OX40 is predominantly expressed on activated $CD4^+$ and $CD8^+$ T cells. OX40 signaling promotes T cell survival, division and cytokine production [17]. In the current study, HFD-fed obese mice exhibited impaired glucose tolerance and IR. Obese mice additionally displayed increased splenic and adipose tissue OX40 and OX40L mRNA expression. Flow cytometric analysis demonstrated higher proportions of OX40 on $CD4^+$ T cells, but not $CD8^+$ T cells, in VAT. Consistent with these results, OX40 gene deletion downregulated CD69 and CD44, the activation markers expressed on $CD4^+$ T cells, but not $CD8^+$ T cells, in VAT and significantly attenuated $CD4^+$ T cell proliferation but not $CD8^+$ T cell proliferation. Furthermore, OX40-KO mice fed HFDs exhibited remarkably decreased IFN-γ-producing $CD4^+$ T cell percentages but not IFN-γ^+ $CD8^+$ T cell percentages in VAT compared to those of HFD-fed WT mice. Differences in OX40 expression between $CD4^+$ and $CD8^+$ T cells have also been observed in other inflammatory situations, with OX40 expression shown to be transient on $CD8^+$ T cells but prolonged on $CD4^+$ T cells [17, 22–24].

In naïve $CD4^+$ T cells, OX40 engagement can lead to either Th1 or Th2 cell generation, depending on the microenvironment in which the cells are located [25–27]. OX40 signaling promotes T cell survival and cytokine production [17]. In our study, we confirmed that in diet-induced obese mice, adipocyte-derived leptin stimulated $CD4^+$ T cells to differentiate into Th1 cells, and OX40 expression enhanced Th1 polarization and IFN-γ secretion further in vitro. Consistent with these findings, HFD-fed WT mice exhibited upregulated *Tbx21, RORγT* transcription factor expression, but not *Gata3* transcription factor expression, in VAT. However, OX40 depletion notably suppressed *Tbx21* expression, but not *Gata3* or *RORγT* expression, which led to significantly decreased percentages of IFN-γ producing $CD4^+$ T cells in adipose tissue. OX40 depletion also partially decreased IL-17 producing $CD4^+$ T cells in adipose tissue as determined by flow cytometry, suggesting that OX40 may also enrolled in Th17 differentiation.

$CD4^+$ $Foxp3^+$ Tregs are important negative regulators of VAT inflammation and IR [1, 5, 20, 28, 29]. Treg cell depletion in WT lean mice results in increased proinflammatory cytokine expression in adipose tissue and increased insulin levels. Restoration of VAT Treg/Th1 balance improves long-term glucose and insulin homeostasis [11]. Costimulation signals are essential for $Foxp3^+$ Treg development and function [30]. The CD28-B7 and CD40–CD40L interactions not only promote effector T cell activation but also maintain Treg development and homeostasis, representing a complex network of receptor-ligand interactions that qualitatively and quantitatively influence immune responses. Blocking the CD28-B7 and CD40–CD40L interactions has been shown to impair Treg proliferation and function and lead to excessive proinflammatory macrophage infiltration and DIO and IR development [9, 31–33].

OX40 is also expressed by $Foxp3^+$ Tregs. However, in contrast to CD28-B7 and CD40–CD40L signaling, OX40–OX40L signaling profoundly abrogated Treg suppressive activity in our study, although OX40 promoted Treg expansion. These findings are also supported by those of other groups using different models [25, 34, 35].

Winer et al. proposed that $CD4^+$ T lymphocytes play a fundamental role in the regulation of body weight, adipocyte hypertrophy, insulin resistance and glucose tolerance in DIO. $CD4^+$ T cells control of glucose homeostasis is compromised in DIO progression, when VAT accumulates pathogenic IFN-γ-secreting Th1 cells, overwhelming static numbers of Th2 and regulatory $Foxp3^+$ Tregs. $CD4^+$ (but not $CD8^+$) T cell transfer into lymphocyte-free Rag1-null DIO mice reversed weight gain and insulin resistance, predominantly through Th2 cells and Tregs [11]. Macrophage numbers and/or proinflammatory gene expression in adipose tissue are positively associated with adipocyte size in obese mice and are negatively associated with weight loss in obese humans [36]. In obesity, inflammation of white adipose tissue is associated with diminished generation of beige adipocytes that express the uncoupling protein UCP1. The *Ucp1* expression in adipocytes was significantly lower when adipocytes cultured in direct contact with proinflammatory macrophages derived from obese adipose tissue and stimulated with LPS plus IFN-γ [37]. In this study, the mechanism by which OX40 deletion decreases adipocyte size and adipose tissue weight could be explained by OX40 may indirect affect white adipocytes differentiation, function and beige adipogenesis through its regulation on Th1 and M1 macrophages.

Comparisons between HFD-fed WT and OX40-KO mice showed that OX40 induced increases in the percentages of Foxp3-positive cells with impaired suppressive activity. Moreover, OX40 induced significant increases in the percentages of IFN-γ-producing cells, resulting in substantially elevated Th1/Treg and M1/M2 macrophages ratios in the VAT of HFD-fed mice and leading to DIO and IR. OX40 deletion significantly reduced Th1 cells and M1 macrophages percentages, restored Treg suppressive activity, rescued immune homeostasis in VAT and attenuated DIO and IR.

To investigate the relevance of our findings to humans, we measured OX40 and OX40L expression in human PBMCs via flow cytometry and real-time PCR. Interestingly, we observed that individuals with higher BMIs exhibited significantly higher OX40 expression on T cells than that of individuals with lower BMIs. These findings indicate that OX40 may play an important role in human obesity.

In summary, VAT $CD4^+$ T cells are activated by adipocytes and leptin in DIO. Together with leptin, OX40 expression enhances $CD4^+$ T cell proliferation, promotes $CD4^+$ T cell differentiation to Th1 cells, increases the Th1/Treg ratio and induces immune invasion in HFD-fed mice. IFN-γ produced by Th1 cells then polarizes adipose tissue macrophages to the M1 phenotype. M1 macrophages subsequently secrete proinflammatory cytokines, which promote adipose tissue inflammation and IR development.

Conclusions

Our study has presented a new mechanism by which OX40, a costimulatory molecule, regulates obesity-related adipose tissue inflammation and IR. Therefore, the OX40 signaling pathway may be a new target in obesity-related IR treatment.

Acknowledgements This work was supported by Grants from the National Natural Science Foundation of China (No. 81500598 and 81501379), Beijing Natural Science Foundation (No. 7162051, 7172060), Beijing Health System Talents Plan (2013-2-026), and the Open Project of Beijing Key Laboratory of Tolerance Induction and Organ Protection in Transplantation (2015YZNS04).

Author contributions BL, HY and GS participated in performing the research, analyzing the data and initiating the original draft of the article. XS, HJ, CZ, DT, WS, KL, HX, XL and JY participated in performing the research and collecting the data. DZ and XH established the hypotheses, supervised the studies, analyzed the data and co-wrote the manuscript.

Compliance with ethical standards

Conflict of interest There is no conflict of interests to be declared from all authors.

References

1. Mathis D (2013) Immunological goings-on in visceral adipose tissue. Cell Metab 17(6):851–859. doi:10.1016/j.cmet.2013.05.008

2. Kalupahana NS, Moustaid-Moussa N, Claycombe KJ (2012) Immunity as a link between obesity and insulin resistance. Mol Aspects Med 33(1):26–34. doi:10.1016/j.mam.2011.10.011
3. Ouchi N, Parker JL, Lugus JJ, Walsh K (2011) Adipokines in inflammation and metabolic disease. Nat Rev Immunol 11(2):85–97. doi:10.1038/nri2921
4. Gregor MF, Hotamisligil GS (2011) Inflammatory mechanisms in obesity. Annu Rev Immunol 29:415–445. doi:10.1146/annurev-immunol-031210-101322
5. Cildir G, Akincilar SC, Tergaonkar V (2013) Chronic adipose tissue inflammation: all immune cells on the stage. Trends Mol Med 19(8):487–500. doi:10.1016/j.molmed.2013.05.001
6. McNelis JC, Olefsky JM (2014) Macrophages, immunity, and metabolic disease. Immunity 41(1):36–48. doi:10.1016/j.immuni.2014.05.010
7. Kintscher U, Hartge M, Hess K, Foryst-Ludwig A, Clemenz M, Wabitsch M, Fischer-Posovszky P, Barth TF, Dragun D, Skurk T, Hauner H, Bluher M, Unger T, Wolf AM, Knippschild U, Hombach V, Marx N (2008) T-lymphocyte infiltration in visceral adipose tissue: a primary event in adipose tissue inflammation and the development of obesity-mediated insulin resistance. Arterioscler Thromb Vasc Biol 28(7):1304–1310. doi:10.1161/ATVBAHA.108.165100
8. Lee BC (1842) Lee J (2014) Cellular and molecular players in adipose tissue inflammation in the development of obesity-induced insulin resistance. Biochim Biophys Acta 3:446–462. doi:10.1016/j.bbadis.2013.05.017
9. Seijkens T, Kusters P, Chatzigeorgiou A, Chavakis T, Lutgens E (2014) Immune cell crosstalk in obesity: a key role for costimulation? Diabetes 63(12):3982–3991. doi:10.2337/db14-0272
10. Deng T, Lyon CJ, Minze LJ, Lin J, Zou J, Liu JZ, Ren Y, Yin Z, Hamilton DJ, Reardon PR, Sherman V, Wang HY, Phillips KJ, Webb P, Wong ST, Wang RF, Hsueh WA (2013) Class II major histocompatibility complex plays an essential role in obesity-induced adipose inflammation. Cell Metab 17(3):411–422. doi:10.1016/j.cmet.2013.02.009
11. Winer S, Chan Y, Paltser G, Truong D, Tsui H, Bahrami J, Dorfman R, Wang Y, Zielenski J, Mastronardi F, Maezawa Y, Drucker DJ, Engleman E, Winer D, Dosch HM (2009) Normalization of obesity-associated insulin resistance through immunotherapy. Nat Med 15(8):921–929. doi:10.1038/nm.2001
12. Bertola A, Ciucci T, Rousseau D, Bourlier V, Duffaut C, Bonnafous S, Blin-Wakkach C, Anty R, Iannelli A, Gugenheim J, Tran A, Bouloumie A, Gual P, Wakkach A (2012) Identification of adipose tissue dendritic cells correlated with obesity-associated insulin-resistance and inducing Th17 responses in mice and patients. Diabetes 61(9):2238–2247. doi:10.2337/db11-1274
13. Morris DL, Cho KW, Delproposto JL, Oatmen KE, Geletka LM, Martinez-Santibanez G, Singer K, Lumeng CN (2013) Adipose tissue macrophages function as antigen-presenting cells and regulate adipose tissue $CD4^+$ T cells in mice. Diabetes 62(8):2762–2772. doi:10.2337/db12-1404
14. Wu H, Perrard XD, Wang Q, Perrard JL, Polsani VR, Jones PH, Smith CW, Ballantyne CM (2010) CD11c expression in adipose tissue and blood and its role in diet-induced obesity. Arterioscler Thromb Vasc Biol 30(2):186–192. doi:10.1161/ATVBAHA.109.198044
15. Cho KW, Morris DL, DelProposto JL, Geletka L, Zamarron B, Martinez-Santibanez G, Meyer KA, Singer K, O'Rourke RW, Lumeng CN (2014) An MHC II-dependent activation loop between adipose tissue macrophages and $CD4^+$ T cells controls obesity-induced inflammation. Cell Rep 9(2):605–617. doi:10.1016/j.celrep.2014.09.004
16. Chen L, Flies DB (2013) Molecular mechanisms of T cell co-stimulation and co-inhibition. Nat Rev Immunol 13(4):227–242. doi:10.1038/nri3405
17. Croft M (2010) Control of immunity by the TNFR-related molecule OX40 (CD134). Annu Rev Immunol 28:57–78. doi:10.1146/annurev-immunol-030409-101243
18. Olefsky JM, Glass CK (2010) Macrophages, inflammation, and insulin resistance. Annu Rev Physiol 72:219–246. doi:10.1146/annurev-physiol-021909-135846
19. Lord GM, Matarese G, Howard JK, Baker RJ, Bloom SR, Lechler RI (1998) Leptin modulates the T-cell immune response and reverses starvation-induced immunosuppression. Nature 394(6696):897–901. doi:10.1038/29795
20. Sell H, Habich C, Eckel J (2012) Adaptive immunity in obesity and insulin resistance. Nat Rev Endocrinol 8(12):709–716. doi:10.1038/nrendo.2012.114
21. Chng MH, Alonso MN, Barnes SE, Nguyen KD, Engleman EG (2015) Adaptive immunity and antigen-specific activation in obesity-associated insulin resistance. Mediat Inflamm 2015:593075. doi:10.1155/2015/593075
22. Gramaglia I, Jember A, Pippig SD, Weinberg AD, Killeen N, Croft M (2000) The OX40 costimulatory receptor determines the development of CD4 memory by regulating primary clonal expansion. J Immunol 165(6):3043–3050
23. Bansal-Pakala P, Halteman BS, Cheng MH, Croft M (2004) Costimulation of CD8 T cell responses by OX40. J Immunol 172(8):4821–4825
24. Lee SW, Park Y, Song A, Cheroutre H, Kwon BS, Croft M (2006) Functional dichotomy between OX40 and 4-1BB in modulating effector CD8 T cell responses. J Immunol 177(7):4464–4472
25. Croft M, So T, Duan W, Soroosh P (2009) The significance of OX40 and OX40L to T-cell biology and immune disease. Immunol Rev 229(1):173–191. doi:10.1111/j.1600-065X.2009.00766.x
26. Ward-Kavanagh LK, Lin WW, Sedy JR, Ware CF (2016) The TNF receptor superfamily in co-stimulating and co-inhibitory responses. Immunity 44(5):1005–1019. doi:10.1016/j.immuni.2016.04.019
27. Kaur D, Brightling C (2012) OX40/OX40 ligand interactions in T-cell regulation and asthma. Chest 141(2):494–499. doi:10.1378/chest.11-1730
28. Cipolletta D, Kolodin D, Benoist C, Mathis D (2011) Tissular T(regs): a unique population of adipose-tissue-resident $Foxp3^{+-}$ $CD4^+$ T cells that impacts organismal metabolism. Semin Immunol 23(6):431–437. doi:10.1016/j.smim.2011.06.002
29. Winer S, Winer DA (2012) The adaptive immune system as a fundamental regulator of adipose tissue inflammation and insulin resistance. Immunol Cell Biol 90(8):755–762. doi:10.1038/icb.2011.110
30. Bour-Jordan H, Bluestone JA (2009) Regulating the regulators: costimulatory signals control the homeostasis and function of regulatory T cells. Immunol Rev 229(1):41–66. doi:10.1111/j.1600-065X.2009.00775.x
31. Zhong J, Rao X, Braunstein Z, Taylor A, Narula V, Hazey J, Mikami D, Needleman B, Rutsky J, Sun Q, Deiuliis JA, Satoskar AR, Rajagopalan S (2014) T-cell costimulation protects obesity-induced adipose inflammation and insulin resistance. Diabetes 63(4):1289–1302. doi:10.2337/db13-1094
32. Wolf D, Jehle F, Michel NA, Bukosza EN, Rivera J, Chen YC, Hoppe N, Dufner B, Rodriguez AO, Colberg C, Nieto L, Rupprecht B, Wiedemann A, Schulte L, Peikert A, Bassler N, Lozhkin A, Hergeth SP, Stachon P, Hilgendorf I, Willecke F, von Zur Muhlen C, von Elverfeldt D, Binder CJ, Aichele P, Varo N, Febbraio MA, Libby P, Bode C, Peter K, Zirlik A (2014) Coinhibitory suppression of T cell activation by CD40 protects against obesity and adipose tissue inflammation in mice. Circulation 129(23):2414–2425. doi:10.1161/CIRCULATIONAHA.113.008055

33. Yi Z, Bishop GA (2015) Regulatory role of CD40 in obesity-induced insulin resistance. Adipocyte 4(1):65–69. doi:10.4161/adip.32214
34. Vu MD, Xiao X, Gao W, Degauque N, Chen M, Kroemer A, Killeen N, Ishii N, Li XC (2007) OX40 costimulation turns off Foxp3^{+} Tregs. Blood 110(7):2501–2510
35. Xiao X, Gong W, Demirci G, Liu W, Spoerl S, Chu X, Bishop DK, Turka LA, Li XC (2012) New insights on OX40 in the control of T cell immunity and immune tolerance in vivo. J Immunol 188(2):892–901. doi:10.4049/jimmunol.1101373
36. Bai Y, Sun Q (2015) Macrophage recruitment in obese adipose tissue. Obes Rev 16(2):127–136. doi:10.1111/obr.12242
37. Chung KJ, Chatzigeorgiou A, Economopoulou M, Garcia-Martin R, Alexaki VI, Mitroulis I, Nati M, Gebler J, Ziemssen T, Goelz SE, Phieler J, Lim JH, Karalis KP, Papayannopoulou T, Bluher M, Hajishengallis G, Chavakis T (2017) A self-sustained loop of inflammation-driven inhibition of beige adipogenesis in obesity. Nat Immunol 18(6):654–664. doi:10.1038/ni.3728